Radovan Petrović[1], Dragana Vasilski[2], Maja Anđelković[1], Simon A. Sedmak[3], Khaled B. Omran[2], Salem I. Shweka[2]*

STRESS CALCULATION AND DEFORMATION OF TANKS LOADED BY INTERNAL GAS PRESSURE LOCATED IN CITY HEATING PLANTS

PRORAČUN NAPREZANJA I DEFORMACIJA REZERVOARA OPTEREĆENIH UNUTRAŠNJIM PRITISKOM GASA LOCIRANIM U GRADSKIM TOPLANAMA

Originalni naučni rad / Original scientific paper
UDK /UDC:

Rad primljen / Paper received: 12.02.2022

Adresa autora / Author's address:
[1)] University 'Union-Nikola Tesla', Faculty of Information Technology and Engineering, Belgrade, Serbia
email: radovan4700@yahoo.com
[2)] University 'Union-Nikola Tesla', Faculty of Sustainable Development Management, Belgrade, Serbia
[3)] University of Belgrade, Innovation Centre of the Faculty of Mechanical Engineering, Belgrade, Serbia

Keywords
- finite element method (FEM)
- deformation
- cylindrical shell
- gas pressure

Ključne reči
- metoda konačnih elemenata (MKE)
- deformacija
- cilindrični rezervoar
- pritisak gasa

Abstract

The paper presents the procedure for calculating stress in gas pressure tanks using finite shell elements for linear and geometrically nonlinear analysis. Therefore, a procedure has been developed to automatically generate the necessary data for the finite element method (FEM), such as geometry, numbering of elements and nodes, and the determination of forces. Forces are calculated from: pressure difference in relation to external pressure; hydrostatic pressure and gas pressure; and pressure vessel weight. It enables fairly simple and easy use of developed software in everyday practice and provides great opportunities for further upgrading and fundamental determination of the impact on parameters for different types of tanks and pressure containers in general.

Izvod

U radu je prikazan postupak proračuna čvrstoće rezervoara pod pritiskom gasa uz primenu konačnih elemenata omotača za linearnu i geometrijski nelinearnu analizu. Zbog toga je razvijena procedura za automatsko generisanje potrebnih podataka za metodu konačnih elemenata (MKE), kao što su geometrija, numeracija elemenata i čvorova i određivanje sila. Sile se računaju od: razlike pritiska u odnosu na spoljašnji, hidrostatičkog pritiska i pritiska gasa i sopstvene težine. Omogućava se prilično jednostavna i laka upotreba razvijenog softvera u svakodnevnoj praksi i pružaju se velike mogućnosti za dalju nadogradnju i fundamentalno određivanje uticaja pojedinih parametara za različite tipove konstrukcije rezervoara i uopšte kontejnera pod pritiskom.

INTRODUCTION

Depending on the type of reservoir, there are certain standards that define all necessary requirements (such as BS 2654/1973, DIN 4119 Deutsche Normen, API 650 - American Petroleum Institute and SRPS EN 13445-3:2014, /1/). Based on previously presented, we can conclude that designers with existing standards are able to define mainly the geometry of reservoir and technical conditions of the development, including structural integrity assessment, /2-4/. Anyhow, when it is required to verify the stability of the shell or complete reservoir, analytical methods are used with classical patterns from general theory of shells.

Application of general theory of shells leads to rather complex calculations. In calculations applying membrane theory, it is shown that satisfactory results are obtained only for shell parts that are sufficiently distant from the ends, but all conditions regarding the contour and the support area cannot be met.

It is logical that in their calculations, the designers have combined these two theories, taking the solution of membrane theory as the first approximation, and as more accurate, they take into account the bending theory, just to meet the conditions regarding the contour.

New methods in the analysis of structures, such as the finite element method (FEM), /4-9/, with the help of a computer, offer by far greater possibilities in relation to classical ones. In the paper we show the procedure for calculating stresses in the reservoir with the application of finite elements of the shells for linear and geometrically non-linear analysis. Therefore, the procedure for automatic generation of the required data for FEM is developed, such as geometry, numeration of elements and nodes and determination of forces. Forces are calculated from the pressure difference in relation to exterior, hydrostatic, and wind pressure, and self weight.

CYLINDRICAL RESERVOIR UNDER GAS PRESSURE

Let us consider a cylindrical horizontal reservoir loaded only by gas pressure, presented in Fig. 1. Reservoir is made of the shell and two bottoms shaped like a rotation shell. At the junction bottom-shell, in addition to transverse forces P_0 there also appear moments, M_0.

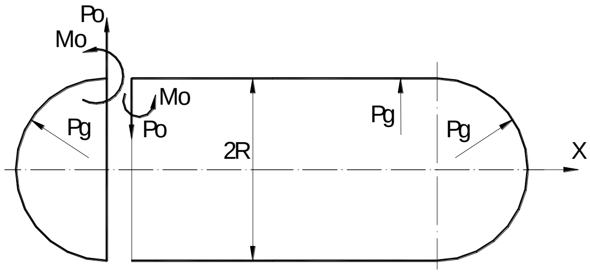

Figure 1. Cylindrical reservoir loaded by internal pressure.

In order to reach the balance equations, we will observe an element cut out from the shell of the reservoir with acting forces, as shown in Fig. 2..

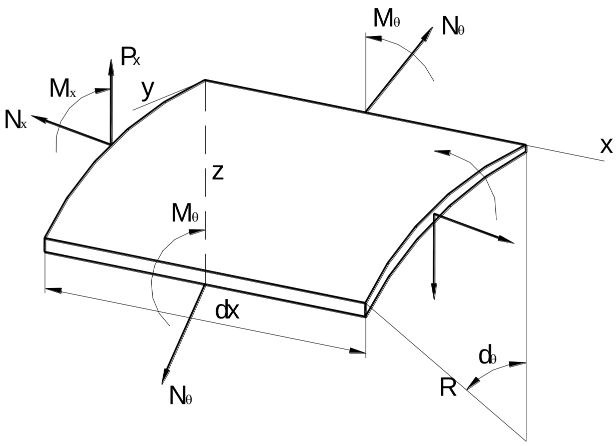

Figure 2. Forces in the cylindrical shell from gas pressure.

Mechanical loads on the shell start only from gas pressure that is normal to the surface, and thus the balance equations are /6/:

In the direction of x axis

$$\frac{dN_x}{dx}dxRd\Theta = 0\,. \tag{1}$$

In the direction of z axis

$$\frac{dP_x}{dx}dxRd\Theta + N_\Theta d\Theta dx - p_g Rd\Theta dx = 0\,. \tag{2}$$

Moments of forces in regard to y axis

$$\frac{dM_x}{dx}dxRd\Theta - P_x dxRd\Theta = 0\,. \tag{3}$$

Moment of force change $dP_x dx/dx$ in relation to the y axis is neglected as a small quantity of higher order.

STRESSES IN CONTAINERS LOADED BY INTERNAL GAS PRESSURE

The membrane theory cannot be fully applied in case of stress analysis of cylindrical containers loaded by internal pressure. Particularly, it cannot be applied at the ends of the cylindrical part of the reservoir, i.e. in the junction bottom-shell. In that case, membrane stresses are followed by local bending stresses, symmetrically distributed in relation to the cylinder axis.

For the sake of illustrating the mentioned state, we shall observe a cylindrical reservoir with the ends in a shape of a hemisphere exposed to external gas pressure p_g.

At a sufficient distance from the junction bottom-shell, the membrane theory gives the following forces per section length unit:

$$N_x = \frac{p_g R}{2} \text{ - longitudinal direction,} \tag{4}$$

$$N_\Theta = p_g R \text{ - circular direction.} \tag{5}$$

For spherical ends, these forces are

$$N_\phi = N_\Theta = \frac{p_g R}{2}\,. \tag{6}$$

Starting from Hooke's law, where

$$\varepsilon_\Theta = \frac{1}{E}(\sigma_\Theta - \mu\sigma_x) = \frac{1}{E\delta}(N_\Theta - \mu N_x)\,, \tag{7}$$

and having in mind that $w = R\varepsilon_\theta$ is the elongation of the cylinder radius, and that

$$\sigma_x = \frac{N_x}{\delta}\,, \quad \sigma_\Theta = \frac{N_\Theta}{\delta}\,,$$

the forces mentioned will cause the following elongations of the cylinder radius.

Elongation of cylindrical shell radius

$$w_1 = \frac{R}{E\delta}\left(p_g R - \mu\frac{p_g R}{2}\right) = \frac{p_g R^2}{E\delta}\left(1 - \frac{\mu}{2}\right), \tag{8}$$

and elongation of spherical shell radius

$$w_2 = \frac{R}{E\delta}\left(\frac{p_g R}{2} - \mu\frac{p_g R}{2}\right) = \frac{p_g R^2}{2E\delta}(1-\mu)\,. \tag{9}$$

From Eqs.(8) and (9), one can see, observing membrane stresses only, that we have a discontinuity /6/. In order to eliminate the discontinuity, it is required to introduce transversal forces P_0 and bending moments M_0, equally distributed at junction bottom-shell, with the condition for their size to be such to eliminate the difference $w_1 - w_2$ of radial extensions given by membrane theory.

Example: stable horizontal 60 m^3 reservoir with propane-butane

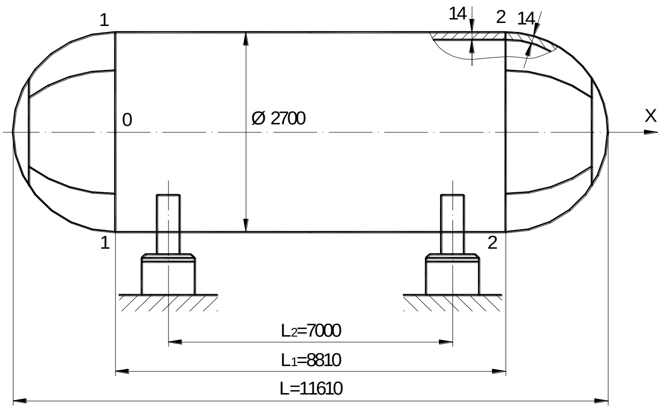

Figure 3. Stable 60 m^3 reservoir for propane-butane gas.

Data: work pressure p_g = 16.7 bar; test pressure $p_g{}'$= 25 bar; bottoms shaped in a hemisphere; wall thickness = shell thickness δ = 14 mm; length of cylindrical part L_1 = 8910 mm; diameter of reservoir R = 1350 mm; range of supports L_2 = 7000 mm.

Values of deflection for particular sections under the impact of transversal force P_0 are given in Table 1.

Table 1. Deflection for particular sections under the impact of transversal force P_0.

Section	x (cm)	w (cm)
1-1	0	-0.0259
2-2	2	-0.0211
3-3	4	-0.0166
4-4	6	-0.0125
5-5	8	-0.0090
5'-5'	8.4	0.00835
6-6	10	-0.0060
7-7	12	-0.0036
8-8	14	-0.0018
9-9	16	-0.00043
10-10	18	0.00053
10'-10'	19.78	0.00114
11-11	20	0.00117
12-12	22	0.00153
13-13	26	0.00172
14-14	30	0.00146
15-15	32	0.00128
16-16	34	0.00106
17-17	40	0.00051
18-18	45	0.00019
19-19	50	0.000009
20-20	55	-0.000060
21-21	65	-0.000058
22-22	75	-0.000017

From Table 1 the highest value of the deflection is below the transversal force at the location of junction bottom-shell. Moving on from that junction towards the middle of the reservoir the deflection has less value, and practically at a distance greater than 75 cm it becomes negligible. Based on this we conclude that the bending moment depends on the section x. For particular sections, the values of bending moment are given in Table 2. From Table 2 we can see that the maximal bending moment is at distance:

$$x=\frac{\pi}{4\lambda}=8.4\text{ cm},\ (M_x)_{\max} = 76.993 \text{ daNcm/cm}$$

Table 2. Values of bending moment.

Section	x (cm)	$M_x = 238.783e^{-\lambda x}\sin\lambda x$
1-1	0	0
2-2	2	36.819
3-3	4	60.017
4-4	6	72.489
5-5	8	76.870
5'-5'	8.4	76.993
6-6	10	75.313
7-7	12	69.919
8-8	14	62.274
9-9	16	53.338
10-10	18	43.837
10'-10'	19.78	35.210
11-11	20	35.138
12-12	22	26.98
13-13	26	13.691
14-14	30	4.77
15-15	32	1.783
16-16	34	-0.371
17-17	40	-3.187
18-18	45	-3.11
19-19	50	-2.231
20-20	55	-1.259
21-21	65	-1.121
22-22	75	0.143

Moving on towards the middle of the reservoir, the bending moment drops and can be neglected at $x > 75$ cm.

Stress discontinuity in the axial direction depends on the bending moment M_x and is given by:

$$\sigma''_x=\frac{6M_x}{\delta^2}=\frac{6M_x}{1{,}4^2}=3.06M_x\ .$$

Values of stress discontinuity for particular sections are given in Table 3 and are calculated based on values of the bending moment given in Table 2.

As we can see from Table 3, the largest value of stress discontinuity is in section 5'-5' i.e. at the location of maximal bending moment. Based on Table 3, we have drawn a diagram (Fig. 4c) that shows the flow of stress discontinuity further from the junction bottom-shell.

Table 3. Values of stress discontinuity for particular sections.

Section	$\sigma_x = 3.06M_x$
1-1	0
2-2	112.666
3-3	183.652
4-4	221.816
5-5	235.222
5'-5'	235.598
6-6	230.458
7-7	213.952
8-8	190.558
9-9	163.214
10-10	134.141
11-11	107.522
12-12-	82.559
13-13	41.894
14-14	14.596
15-15	5.456
16-16	-1.135
17-17	-9.752
18-18-	-9.516
19-19-	-6.827
20-20	-3.852
21-21	-3.430
22-22	0.437

Membrane stress in axial direction

Membrane stress in axial direction of cylindrical part of the reservoir is:

$$\sigma'_x=\frac{p_g R}{2\delta}=\frac{16.7\cdot 135}{2\cdot 1.4}=805.178\text{ daN/cm}^2\ .$$

Maximal stress in axial direction

The maximal stress value in the axial direction is obtained by adding membrane stress to the highest value of stress discontinuity in that direction, i.e.

$$(\sigma_x)_{\max}=\sigma''_x+\sigma'_x=235.598+805.178=1040.77\text{ daN/cm}^2\ .$$

Putting into relation: $(\sigma_x)_{\max}/\sigma_x' = 1.292$, we conclude that the maximal stress is ≈ 30 % greater than for the membrane, which is caused precisely by the discontinuity stress in section 5'-5'. The stress diagram in axial direction is given in Fig. 4a.

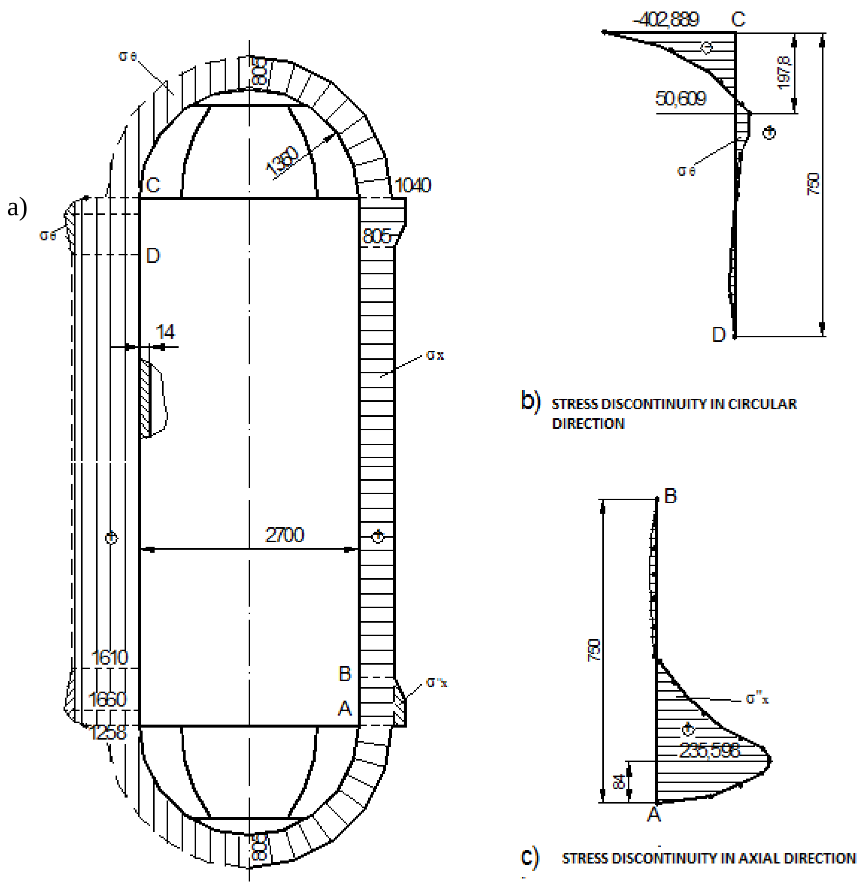

Figure 4. Cylindrical reservoir with ends shaped as hemisphere, loaded only by gas pressure.

Stress discontinuity in circular direction

Stress discontinuity in the circular direction is caused by deflection w, and the bending moment at surrounding locations of junction bottom-shell is given by:

$$\sigma'_\Theta = \frac{Ew}{R} + \frac{6\mu}{\delta^2} M_x .$$

In the specific case it will be:

$$\sigma''_\Theta = \frac{2100000}{135} w + \frac{6\cdot 0.3}{1.4^2} M_x ,$$

$$\sigma'_\Theta = 15555.556 w + 0.918 M_x .$$

Using the values of deflection and moments, the values of σ_Θ'' are calculated and presented in Table 4.

From Table 4, one can see that the highest value of stress discontinuity is in section 1-1. The second extreme value is in section 10'-10', i.e. for $x = 1.858/\lambda = 19.78$ cm.

Stress discontinuity further from this section, towards the middle of the reservoir is dropping, which can be seen from the diagram in Fig. 4b.

Table 4. Values of σ_Θ''.

Section	σ_Θ''	Section	σ_Θ''
1-1	-402.889	12-12	48.567
2-2	-294.422	13-13	39.324
3-3	-203.126	14-14	27.09
4-4	-127.899	15-15	21.548
5-5	-64.590	16-16	16.148
6-6	-24.196	17-17	5.007
7-7	8.185	18-18	0.100
8-8	29.167	19-19	-1.908
9-9	42.275	20-20	-2.089
10-10	48.487	21-21	-2.002
10'-10'	50.609	22-22	-1.241
11-11	50.456		

Membrane stress in circular direction

Membrane stress of the cylindrical part of reservoir in circular direction, under the effect of internal gas pressure:

$$\sigma'_\Theta = \frac{p_g R}{\delta} = \frac{16.7\cdot 135}{1.4} = 1610.357 \text{ daN/cm}^2 .$$

Maximal stress in circular direction

The maximal stress in circular direction is obtained by adding membrane stress of the highest positive value of stress discontinuity, in this case with stress in section 10'-10'

$$(\sigma_\Theta)_{max} = \sigma'_\Theta + \sigma''_\Theta = 1610.35 + 50.60 = 1660.96 \text{ daN/cm}^2 .$$

Putting into the relation:

$$(\sigma_\Theta)_{max}/\sigma_\Theta' = 1660.966/1610.357 = 1.031,$$

it is shown that membrane stress is 3 % less than maximal stress in the circular direction in section 10'-10'.

The stress diagram in the circular direction is shown in Fig. 4a.

Membrane stresses in spherical ends of the reservoir

Membrane stresses in the spherical ends are equal both in the circular and meridian direction, and they are:

$$\sigma_\Theta = \sigma_\phi = \frac{p_g R}{2} = 805.178 \text{ daN/cm}^2 .$$

The diagram of membrane stress for spherical ends is shown in Fig. 4a. Analysing the stress diagrams in Fig. 4a-c, one can conclude that for a calculation of the reservoir exposed to internal gas pressure, the stress in the circular direction becomes relevant, because when compared to the stress in the axial direction, it has a higher value. Here we observe the maximal value of circular stress $\sigma_{\Theta max}$ = 1660.966 daN/cm^2 at distance x = 19.78 cm from the junction bottom-shell. We should bear this in mind particularly when the junction bottom-shell is performed by welding, in which case we must predict thermal procedures for eliminating residual welding stresses, otherwise they could be added to the maximal stress.

CONCLUSIONS

According to the influence of internal pressure, tanks can be divided into tanks without pressure (up to 0.5 bar), and tanks under pressure (> 0.5 bar). According to the shape, we can divide them into cylindrical, spherical, and conical tanks. Depending on the position of the axis of symmetry, the tanks can be horizontal or vertical.

In the design of tanks and pressurized containers in general, the stress calculation is very important. There are various procedures by which we can determine with greater or lesser accuracy the desired quantities that define the behaviour of the structure. Significant efforts in solving this task have led to standardised procedures, and recommendations and standards in the field of reservoir design.

By applying the finite element method (FEM) and experimental tests of tank strength, it is possible to optimise structural materials of the tank shell and their supports. The standards also stipulate the quality of materials for the construction of tanks, with special emphasis on mandatory control and testing of the same. As an illustration of the application of the developed procedures, solutions of some derived structures are shown. It provides a rather simple and easy usage of the developed software in everyday practice and provides great opportunities for further upgrade and fundamental determination of the impact of particular parameters for different types of reservoir structures, and generally, containers under pressure.

ACKNOWLEDGEMENTS

Some of the studies are supported by the Ministry of Education, Science and Technological Development of the Republic of Serbia, grants TR 32036 and TR 35038.

REFERENCES

1. Milovanović, A., Sedmak, A., Tomić, R., et al. (2016), *Calculation of local loads in torispherical end of vertical vessel with skirt according to EN 13445-3:2014*, Struct. Integ. Life, 16(1): 53-58.
2. Jeremić, L., Sedmak, A., Milovanović, A., et al. (2021), *Assessment of integrity of pressure vessels for compressed air*, Struct. Integ. Life, 21(1): 3-6.
3. Milovanović, A.M., Mijatović, T., Diković, Lj., et al. (2021), *Structural integrity analysis of a cracked pressure vessel*, Struct. Integ. Life, 21(3): 285-289.
4. Medjo, B., Arsić, M., Mladenović, M., et al. (2020), *Influence of defects on limit loads and integrity of the pipeline at Hydropower Plant 'Pirot'*, Struct. Integ. Life, 20(1): 82-86.
5. Milovanović, A.M., Martić, I., Trumbulović, Lj., et al. (2021), *Finite element analysis of spherical storage tank stress state*, Struct. Integ. Life, 21(3): 273-278.
6. Petrović, R., Kojić, M., Đorđević, D., Design of Tanks for Storage and Transport of Fluids (in Serbian: Projektovanje rezervoara za skladištenje i transport fluida), University of Kragujevac, Faculty of Mechanical Engineering Kraljevo, 2005. ISBN 86-82631-21-0
7. Kojić, M. (2002), *An extension of 3-D procedure to large strain analysis of shells*, Comp. Meth. Appl. Mech. Eng. 191(23-24): 2247-2462. doi: 10.1016/S0045-7825(01)00367-X
8. Wang, Z.R, Yushan, Z., Yuansong, Z., Shijian, Y. (1996), *Experimental research and finite-element simulation of plates hidrobulging in pairs*, Int. J Pres. Ves. Piping, 68(3): 243-248. doi: 10.1016/0308-0161(95)00073-9
9. Kaptan, A., Kisioglu, Y. (2007), *Determination of burst pressures and failure locations of vehicle LPG cylinders*, Int. J Pres. Ves. Piping, 84(7): 451-459. doi: 10.1016/j.ijpvp.2007.02.004